

Modelling the interaction between ethnicity and infectious disease transmission dynamics

Vincent X. Lomas^{ab}, and Tim Chambers^b, Michael J. Plank^a

^aSchool of Mathematics and Statistics, University of Canterbury, Christchurch, Aotearoa;

^bNgāi Tahu Research Center, University of Canterbury, Christchurch, Aotearoa

ARTICLE HISTORY

Compiled July 16, 2025

ABSTRACT

During the COVID-19 pandemic, Aotearoa followed an elimination strategy followed by a mitigation strategy, which saw high success and kept health impact low. However, there were inequities in health outcomes, notably that Māori and Pacific Peoples had lower vaccine coverage and experienced higher age-standardised rates of hospitalisation and death. Models provide predictions of disease spread and the burden of disease, which can effectively inform policy, but are often not good at including inequities/heterogeneity. Despite the differences in health outcomes by ethnicity, most models have not explicitly considered ethnic heterogeneities as factors. We developed such a model to investigate the first Omicron wave of the COVID-19 pandemic in Aotearoa, which was the first time there was widespread community transmission of SARS-CoV-2. We analysed three models for contact patterns within and between ethnicities—proportionate mixing, assortative mixing, and empirically derived mixing—and fit them using ethnicity-specific data on reported cases and spatially disaggregated population counts. We found that Māori, Pacific, and Asian contact rates were between 1.17-2.46, 1.60-3.89, and 0.83-0.92 times the European rates, respectively. We then found that from the parameters considered in the model, the disparity in transmission rates explained the majority of the observed disparity in attack rates, while assortativity and vaccine rates explained comparably less.

Abbreviations: SA1 - Statistical area 1, SA2 - Statistical area 2, CAR - Case Ascertainment Rate, PCR - Polymerase Chain Reaction, RAT - Rapid Antigen Test

KEYWORDS

mathematics; mathematical modelling; epidemiology; health equity; COVID-19; compartmental model;

1. Introduction

When the COVID-19 pandemic began in 2020, it was predicted that Māori would be disproportionately affected [1], with one model estimating that the COVID-19 infection fatality rates would be 50% higher for Māori compared to non-Māori [2]. A combination of living conditions, lack of access to quality health care, and existing health conditions led to Māori having a higher risk of infection and developing more serious symptoms of COVID-19 [3]. During the first Omicron wave, Māori and Pacific Peoples had the highest per capita rates of cases and hospitalisations, with odds ratios of hospitalisation

of 2.03 and 1.75 for Māori and Pacific Peoples, respectively [4]. This was consistent with historical inequities in infectious disease burden experienced by Māori and Pacific Peoples [5–10].

During the COVID-19 pandemic, Aotearoa changed its policy approach to COVID-19 at multiple stages. Aotearoa initially responded to the spread of COVID-19 with an elimination strategy. The elimination strategy aimed to completely eliminate COVID-19 from the country. This approach worked and resulted in about 30 cases and 0.4 deaths per hundred thousand population by August 2020 [11]. When vaccines became widely available, a mitigation strategy was used instead [12]. Starting in February, 2021, COVID-19 vaccines began to be administered to border and managed isolation and quarantine workers [13] and then the public thereafter. From March to May 2021, there was a large gap in the proportion of vaccinated Māori and Pacific Peoples compared to other ethnicities. At this time, the government implemented the mitigation strategy via the "traffic light" system formally known as the COVID-19 Protection Framework. This framework implemented social distancing requirements, mask mandates, and COVID-19 vaccination certificates and their requirements [14]. From May 2020 until the Omicron waves started in January 2022, there was very little community transmission. Starting in 2022, when there was high vaccination coverage [15], there was some transmission of Omicron cases from isolation facilities at the border where international arrivals were being isolated. This resulted in a major wave that peaked on February 25th, 2022, with 24,226 daily confirmed cases. After this, the borders were reopened, and international travel was allowed in March 2022. Starting in July, an influx of immune-evasive variants was observed through the border. Most of these cases did not result in detected community transmission; a small amount did, resulting in large outbreaks [16]. Although the first and second doses of the vaccine had reduced efficacy against the Omicron variant compared to previous variants, it was shown that the booster doses were effective at stopping severe disease [17].

Models add a lot of value to predictions of the spread and burden of disease and can effectively inform policy for prevention measures but are often not very good at including inequities/heterogeneity. Without these considerations, the models cannot address or predict these issues as effectively. Previous models have often struggled to account for ethnic heterogeneities despite their effect on disease spread [18], which has limited their ability to assess health equity. There are many models that use socioeconomic status [19] or age [20–22] as factors, but models that consider ethnicity as a factor [23,24] are rarer. The mathematical models that were used to inform the Aotearoa policy approach to COVID-19 lacked the capability to adequately answer questions about health inequities and policy effectiveness. This limitation was identified as a major gap in the literature in these policy informing works [25,26]. As such, there is a need to develop models that can answer these questions and consider a greater number of heterogeneities.

A method developed by Ma et al. fit considered ethnicity explicitly using data from Long Island and New York City during late April, 2020 [23]. In this paper, they used a compartmental model and split the population into five ethnicity sub-groups: non-Hispanic white, Hispanic or Latino, non-Hispanic Black/African American, non-Hispanic Asian, and Multiracial/Other. Contact patterns were estimated using an ethnicity-specific contact rate, which was the average number of people interacted with each day, and an assortativity constant, ϵ , which measured the extent to which people are more likely to contact other people of the same ethnicity. Their model was first fit to a cross-sectional serosurvey from New York in late April 2020, using a proportionate mixing assumption ($\epsilon = 0$), where people met according to population sizes and ethnicity-specific contact rates with no preference for interacting with any ethnic-

ity. From this fit it was found that minorities, such as Hispanics or Latinos and non-Hispanic Black/African Americans, had higher contact rates compared to non-Hispanic white people, with contact rates in New York City being 2.25, 1.62, 0.86, and 1.28 times the non-Hispanic white rate for Hispanic or Latino, non-Hispanic Black/African American, non-Hispanic Asians, and Multiracial/Other, respectively.

Ma et al. then estimated a value for the assortativity constant based on the extent to which people of the same ethnicity tend to be clustered together in the same census blocks, with an assumption of density-based proportionate mixing within each block. This process gave more weight to the ethnic distribution of higher population blocks. The assortativity constant was chosen to minimise the difference between a census-informed matrix and a matrix formed using the total populations and the assortativity constant. The result of this fit was that 46% and 39% of an ethnicity's contacts were purely intra-ethnic contact in New York and Long Island, respectively; the disparity in contact rates was lowered to 1.62, 1.35, 0.90, and 1.17 times the non-Hispanic rate in New York City for Hispanic or Latino, non-Hispanic Black/African American, non-Hispanic Asians, and Multiracial/Other, respectively, but the disparity in rates was still present.

Here, we applied a similar method to Ma et al. and aimed to estimate ethnicity-specific contact patterns by fitting a model to data on confirmed cases of COVID-19 during Aotearoa's first Omicron wave in 2022. We also aimed to try and understand the relative contributions of different drivers (vaccination rates, contact rates, and assortative contact patterns) to observed trends. We made two main adjustments to the Ma et al. method: we considered a vaccinated population in addition to an unvaccinated population and we changed the way contacts were estimated within census blocks, which allowed us to work directly with the census inform matrix. We then applied our model to the first Omicron wave in Aotearoa to analyse differences in transmission rate by ethnicity. These transmission rates were then used as parameters to investigate various scenarios to analyse the spread of COVID-19 in the model.

2. Methods

In a closed, homogeneous population, an infectious disease can be modelled by a system of differential equations known as the SEIR model:

$$\frac{dS}{dt} = -\beta SI \quad (1)$$

$$\frac{dE}{dt} = \beta SI - \sigma E \quad (2)$$

$$\frac{dI}{dt} = \sigma E - \gamma I \quad (3)$$

$$\frac{dR}{dt} = \gamma I \quad (4)$$

where S, E, I, and R refer to the susceptible, exposed, infectious, and recovered populations, respectively. We set the mean latent period, $1/\sigma$, to 3 days and the mean infectious period, $1/\gamma$, to 4 days to match the Ma et al. study. There is some evidence that the Omicron variant had a shorter latent and infectious period than the wild-type variant [27]. However, as we are mainly interested in cumulative attack rates here, our results

are not sensitive to choices for these parameters. The per capita transmission rate was defined in terms of the basic reproduction number, R_0 , and the total population, N , $\beta = \gamma R_0 / N$.

We then extended this model in the same way as Ma et al. to incorporate multiple ethnic groups by considering a per capita transmission matrix, β , which governs the rate at which transmission happens within and between the considered ethnic groups. The per capita transmission matrix elements, β_{ij} , were the average proportion of susceptible people in ethnic group i an infectious individual from ethnic group j infected each day. In addition to this (beyond the Ma et al. extension), we also considered a susceptible vaccinated group, S_v , and redefined S to be the unvaccinated susceptible group.

$$\frac{d\mathbf{S}}{dt} = -(\beta\mathbf{I}) \circ \mathbf{S} \quad (5)$$

$$\frac{d\mathbf{S}_v}{dt} = -(1 - v_e)(\beta\mathbf{I}) \circ \mathbf{S}_v \quad (6)$$

$$\frac{d\mathbf{E}}{dt} = (\beta\mathbf{I}) \circ \mathbf{S} + (1 - v_e)(\beta\mathbf{I}) \circ \mathbf{S}_v - \sigma\mathbf{E} \quad (7)$$

$$\frac{d\mathbf{I}}{dt} = \sigma\mathbf{E} - \gamma\mathbf{I} \quad (8)$$

$$\frac{d\mathbf{R}}{dt} = \gamma\mathbf{I} \quad (9)$$

In these equations, v_e refers to the vaccine effectiveness, which we set to be 0.3, as it has been shown that the vaccines had reduced effectiveness against infection via Omicron [28]; \circ denotes element-wise multiplication; and \mathbf{S} , \mathbf{S}_v , \mathbf{E} , \mathbf{I} , and \mathbf{R} denote column vectors containing the compartmental populations for each group. The ethnic groups considered were Māori, Pacific Peoples, Asian people, and European/Others, as they are the major ethnic groups within Aotearoa and are consistently identified in health and population data and were identified in our data [15,29–31].

2.1. Transmission matrix

We defined the per capita contact matrix using a similar method to Ma et al. [23]. We considered that on average, each ethnic group interacted with a different number of people per day; this was modelled with an ethnicity-specific contact rate, \hat{a}_k , where k denoted the ethnicity. We assumed that the proportion q of contacts resulting in infection was the same for all ethnicities. We define the transmission vector as $\mathbf{a} = q\hat{\mathbf{a}}$. The transmission vector was the average number of people infected per day by an infectious person in a fully susceptible population. The differences in transmission rates between ethnicities are interpreted as being caused by differences in contact rates, i.e. social factors, not biological factors. Using this definition, q and \hat{a}_k were not separately identifiable, and so we expressed the model in terms of \mathbf{a} and aimed to estimate \mathbf{a} by fitting the model to data as described below.

2.1.1. Proportionate mixing

We first explored the simplest case that assumed each person's contacts were distributed across ethnicity groups in proportion to their population size. This defined each element of the per capita transmission matrix as proportional to the transmission rates of two ethnicities multiplied together, as seen in Equation 10. This left four parameters to fit,

the values of a_k .

$$\beta_{ij, \text{prop mix}} = \frac{a_i a_j}{\sum_k a_k N_k} \quad (10)$$

The population of ethnic group k is represented with N_k .

2.1.2. Assortative mixing

We then considered a more realistic representation of transmission by accounting for preferential interaction within ethnicities with the introduction of the assortativity coefficient, $\epsilon \in [0, 1]$, which was the same for all ethnicities. $\epsilon = 0$ is proportionate mixing, $\epsilon = 1$ is purely within group, and intermediate values of ϵ interpolate between these two extremes. This helped to model community and family interactions that were primarily intra-ethnic interactions. We then defined the assortative per capita transmission matrix via Equation 11.

$$\beta_{ij, \text{assort}} = (1 - \epsilon) \frac{a_i a_j}{\sum_k a_k N_k} + \epsilon \delta_{ij} \frac{a_i}{N_i} \quad (11)$$

$\delta_{ij} = 1$ if $i = j$ and $\delta_{ij} = 0$ otherwise. As can be seen, swapping i and j does not alter the equation, which means that the per capita transmission matrix was symmetric. From this equation, it can be seen that proportionate mixing was a special case where $\epsilon = 0$.

2.1.3. Initialisation

To initialise the model, we assumed that 0.01% of each ethnicity was exposed to the infection, which gave approximately 500 initially exposed people.

$$\begin{aligned} S_k(0) &= (1 - w)N_k - N_{vk} \\ S_{vk}(0) &= N_{vk} \\ E_k(0) &= wN_k \\ I_k(0) &= R_k(0) = 0 \end{aligned}$$

N_{vk} refers to the vaccinated population of ethnic group k , and $w = 0.0001$ was the initial proportion of the population exposed to the disease.

2.2. Parameter estimation and Data sources

2.2.1. COVID-19 case data

The data for the number of confirmed COVID-19 cases was downloaded from the Populations web tool (30 April, 2025), Health New Zealand, based on customised population projections provided by Stats NZ according to assumptions agreed to by Health New Zealand [30]. This data grouped the number of new cases per ethnicity for each day using a priority measure to assign each case to a single ethnicity (Figure 1), which meant in the case of individuals belonging to more than one ethnic group, their case was assigned in the priority order of Māori, Pacific Peoples, Asian, and finally European/Other. The

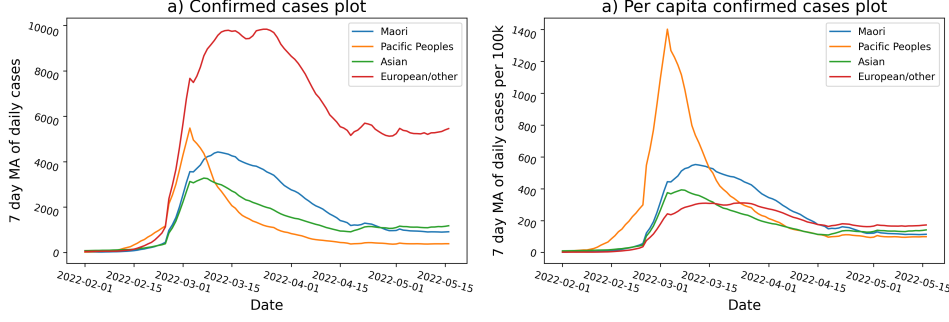


Figure 1. a) 7-day moving average of daily confirmed cases and b) 7-day moving average of confirmed cases per 100k for each ethnicity.

bulk of confirmed cases during the first Omicron wave were self-reported RATs (Rapid Antigen Tests), with some PCR (Polymerase Chain Reaction) tests (for cases presenting to healthcare). We assumed values for the case ascertainment rate (CAR), the proportion of cases that were reported, to account for asymptomatic cases and unreported cases (as the bulk of cases were self reported). As the true values for CAR were not known, we assumed four different situations: equal CARs of 40%, 50%, and 60% across ethnicities, and a situation where Māori and Pacific Peoples reported fewer cases and had a 40% CAR, while Asian and Europeans/Others had a CAR of 60%. We included this scenario as it is possible that Māori and Pacific Peoples had lower testing rates due to factors such as reduced access to healthcare services, higher rates of insecure employment, financial pressure, and/or inability to work remotely. CAR estimates were based on an Aotearoa study from February-July 2022 using wastewater surveillance. In this study, 40% of 20–25-year-olds reported a case, giving an approximate lower bound on CAR, and model comparison to border workers gave an upper bound of around 60% [32]. It can be seen in Figure 1 that there is a sharp increase in the reported Pacific cases present when self-testing became more available. This could imply that a significant portion of early Pacific cases could not be reported due to limited test availability and are therefore missing from the dataset.

2.2.2. Vaccinated population data

The Ministry of Health GitHub repository [15] was used to obtain values for the vaccinated populations for each ethnicity. The dataset contained the number of first doses administered in Aotearoa by the 16th of February, 2022, which was used as the vaccinated population. The proportion of coverage was similar among 1st and 2nd dose numbers, being 57.9%, 76.0%, 75.3%, and 84.4% compared to 55.3%, 74.4%, 74.6%, and 83.4% for Māori, Pacific Peoples, Asians, and Europeans/Other, respectively.

2.2.3. Proportionate mixing estimation

Ethnicity-specific attack rates (i.e., cumulative number of cases per capita) were calculated from the 1st of February to the 16th of May, 2022, to capture the first Omicron wave in Aotearoa. These attack rates were then scaled up using the CAR. The four ethnicity-specific transmission rates, a_k , were estimated by fitting the model to the attack rate data under the proportionate mixing assumption such that the attack rates from the model matched the attack rates from the case data by using the `optimize.fsolve`

Table 1. Table of parameter values.

Symbol	Meaning	Value
β	Per capita transmission matrix	Method dependent
σ	Inverse of latent period	1/3 day ⁻¹
γ	Inverse of infectious period	1/4 day ⁻¹
	cumulative reported cases per capita for ethnic group k	
	Māori	23.9%
	Pacific	30.5%
	Asian	17.1%
	European/Other	18.6%
N_k	Population of ethnic group k	
	Māori	888840
	Pacific	359480
	Asian	820580
	European/Other	3048470
N_{vk}	Vaccinated population of ethnic group k	
	Māori	514930
	Pacific	274413
	Asian	629841
	European/Other	2558007
v_e	Vaccine effectiveness	0.3

function from the SciPy package in Python with its default parameters. All models were fit over a 365-day period, as it allowed sufficient time for the epidemic to run its course.

2.2.4. Area-level population data

Population data for the populations of each ethnic group in specified geographical areas was needed to fit the assortative model. We used ethnicity-stratified population data at two levels of spatial resolution: Statistical Area 1 (SA1) and Statistical Area 2 (SA2). We assumed these areas represented the bulk of interactions for an individual living within that area.

The SA1 regions were formed by joining meshblocks (the smallest administrative unit) to "allow the release of more detailed information about population characteristics..." [33, p. 13]. The SA1 regions have an ideal population range of 100 to 200 people in each region.

The SA2 regions were defined in a way that "aims to reflect communities that interact together socially and economically" [33, p. 14]. SA2 regions have between 1,000 and 4,000 people in them, but in some cases have less than 1,000. As the SA2 blocks were formed to model a community's social interactions, they may appear a more accurate measure. However, a substantial amount of COVID-19 infections occurred within households [34], and as such, the finer-scale grouping of the population that gave more weight to local ethnic distributions may give valuable insights. Statistics for the statistical area datasets used can be seen in Appendix A.

The national ethnic population estimates were found by summing over Te Whatu Ora's District Health Board SA2 populations by prioritised ethnicity [31]. This gave population estimates of 895,040, 363,330, 877,240, and 3,025,980 for Māori, Pacific Peoples, Asians, and Europeans/Others, respectively.

2.2.5. Assortative mixing estimation

Statistical area data was used to select a value for the assortativity constant using a similar method as Ma et al. [23]. The method first constructed an empirically estimated transmission matrix, \mathbf{T}' , using a specified transmission vector, \mathbf{a} , as defined in the following equation:

$$T'_{ij} = \sum_l^L \frac{a_i a_j N_{i,l} N_{j,l}}{\sum_k a_k N_{k,l}} \quad (12)$$

To construct this matrix, a proportionate mixing scheme was applied to the populations of each statistical area to calculate the transmission matrix within that statistical area. The difference between Ma et al.'s method and ours was we assumed frequency-dependent interactions within statistical areas, whereas they assumed density-based interactions in their block groups. Frequency-dependent interactions assume that the mean number of people an individual interacts with each day is constant and does not depend on the population size in the census block or statistical area, while the mean number of density-dependent interactions does. The aggregation over the statistical areas gave the empirically estimated transmission matrix. This was based on an approximating assumption that people mix proportionately with other people in the same geographical area and do not mix with people in other areas. This assumption was not entirely accurate to the real world but gave a good idea of the interactions an individual from each statistical area would have.

\mathbf{a} and ϵ were estimated jointly via an iterative method as follows: For a given \mathbf{a} , we found the value of ϵ that minimised the difference between the empirical matrix \mathbf{T}' and the assortative mixing matrix \mathbf{T} , defined by the following equation:

$$T_{ij} = (1 - \epsilon) \frac{a_i a_j N_i N_j}{\sum_k a_k N_k} + \epsilon \delta_{ij} a_i N_j \quad (13)$$

We did this by solving the following optimisation problem for ϵ :

$$\epsilon = \underset{\hat{\epsilon}}{\operatorname{argmin}} \sum_{i,j} |T_{ij} - T'_{ij}| \quad (14)$$

$$= \underset{\hat{\epsilon}}{\operatorname{argmin}} \sum_{i,j} \left| (1 - \hat{\epsilon}) \frac{a_i a_j N_i N_j}{\sum_k a_k N_k} + \hat{\epsilon} \delta_{ij} a_i N_j - \sum_l^L \frac{a_i a_j N_{i,l} N_{j,l}}{\sum_k a_k N_{k,l}} \right| \quad (15)$$

where $N_{i,l}$ is the population of ethnic group i living in geographic region l . Then, for this value of epsilon, we estimated \mathbf{a} by fitting the model to the attack rate data in the same way as described previously. This iterative process was repeated until the absolute difference between successive values of ϵ was less than 10^{-6} .

2.2.6. Non-parametric mixing estimation

The assortative mixing model allowed for within-group contacts to occur more frequently than under the proportionate mixing model but still assumed that the level of assortativity was the same for all ethnic groups and that inter-ethnic contacts occurred in proportion to population size. To investigate the effects of relaxing this assumption,

Table 2. Table of scenarios to quantify the effects of parameters used in the model.

Scenario	Assortativity constant	Vaccination rate	Transmission rate
1	Fitted value	Ethnicity-specific	Ethnicity-specific
2	Zero	Ethnicity-specific	Ethnicity-specific
3	Fitted value	Population average	Ethnicity-specific
4	Fitted value	Ethnicity-specific	Population average

we directly estimated the transmission matrix using the 4 transmission rates and the statistical area data. We did this by constructing the empirically estimated transmission matrix via Equation 12 and using that to fit a model to the attack rates. This meant only four parameters needed to be estimated, the four transmission rates, leaving one unique fitted solution. The fitted empirically estimated transmission matrix was referred to as the non-parametric transmission matrix due to its non-parametric nature. The use of this matrix was made possible by the change to frequency-based interactions within the SAs.

To conserve the transmission rate definition and symmetry in the per capita matrix, the non-parametric matrix required that the populations used to construct it equal the populations used in the model. This meant the non-parametric matrix was only constructed using the prioritised SA2 data.

2.3. Scenario analysis

We created four scenarios to quantify the effect that the disparity in vaccination, disparity in transmission rates, and the assortativity constant had on model results. These scenarios, seen in Table 2, took the assortative model fit and did one of three things: set ϵ to zero to measure the effect of assortativity on the model; set all transmission rates to the national transmission rates; or set all vaccination rates to the national vaccination rates. These scenarios conserve the total number of vaccinations and the national transmission rates.

3. Results

Code to replicate results can be found in a GitHub repository [35].

3.1. Proportionate mixing

Figure 2 shows the time series of the susceptible, exposed, infectious, and recovered populations for each ethnicity. As expected with an SEIR model, a single epidemic wave that ends as a result of herd immunity in the population was observed. Recall that the transmission rates were fit to match the attack rates observed in the data. As such, the final recovered population in each ethnicity matched the number of people infected according to the attack rate data and the assumed value for CAR (indicated by the dashed horizontal line).

For all the assumed values of CAR, we fit transmission rates to match the new attack values; see Figure 3 and Table 3. For all values of CAR investigated, Pacific Peoples had the highest transmission rate, followed by Māori, Europeans/Others, and then Asians. The initial reproduction number increased with a decrease in the assumed CAR and

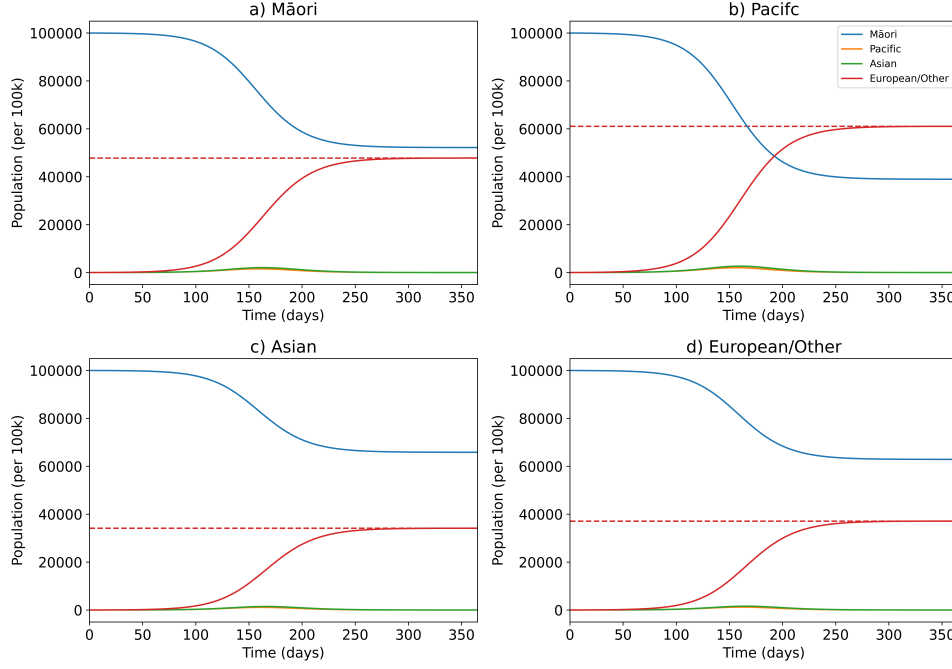


Figure 2. Per capita SEIR plots fit to data on confirmed cases under the assumption of proportionate mixing and an assumed CAR of 50% for a) Māori, b) Pacific Peoples, c) Asians, and d) Europeans/Others. The dashed line is the cumulative attack rate according to the data on reported cases and the assumed CAR of 50%.

was highest when Māori and Pacific Peoples were given a higher CAR than the other groups.

3.2. Assortative mixing

3.2.1. Specified ϵ

We now investigate the inclusion of assortativity in the model to represent preferential inter-ethnicity interactions. There was no immediately obvious choice for the value of assortativity, so we first explored model outputs over the full range of $0 \leq \epsilon \leq 1$ (plots of this are present in Appendix B.). We then estimated the value for assortativity and the transmission rates (Figure 4) using the statistical area data. We present the results for the SA2-prioritised fit here; results for SA1/SA2 total ethnicity are present in Appendix C. The transmission rates fit using the SA1-total and SA2-total data were qualitatively similar, but the SA1-total data had the highest values for ϵ . This was an expected result due to smaller subdivisions sampling a smaller number of people, which increases the assortativity we would expect.

3.2.2. Non-parametric mixing

We now construct the non-parametric transmission matrix directly from the population data, without imposing a particular mixing pattern to eliminate assumptions about national proportional mixing and assortativity. Again, the constructed matrix was fit such that the attack rates from the model match the data. The transmission rates can be seen in Figure 4. When compared to the proportionate mixing rates, the non-parametric

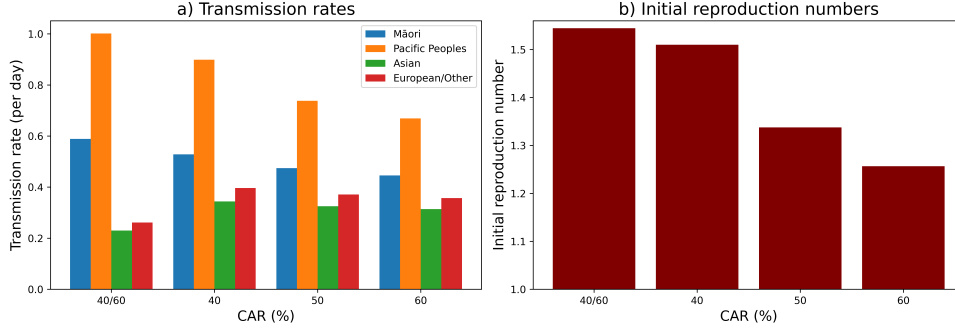


Figure 3. a) Comparison between the transmission rate fits such that the attack rates match the data on confirmed cases for all the assumed CARs under the assumption of proportionate mixing and b) the initial reproduction number for these transmission rates.

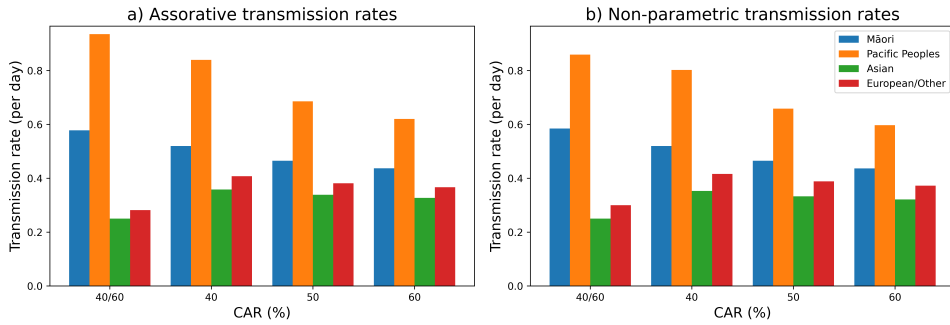


Figure 4. The transmission rates fit to an a) assortative model and b) non-parametric model. The transmission rates were fit such that the attack rates from the model matched the attack rates from the data adjusted with the four CARs considered.

rates for Māori and Pacific rates were lower, while the Asian and European/Other rates were higher, which meant there was a lesser disparity between the rates.

We compared the transmission matrices for the assortative mixing model with the non-parametric model in Figure 5. The matrices remained relatively similar; the elements in the non-parametric matrix were 0.65-1.35 times the values in the assortative matrix, with the biggest difference between methods being the frequency of interaction between the Pacific and the Asian and European/Other groups, which had the biggest relative decrease and increase, respectively. All Pacific interactions increased except for the Pacific-European/Other interaction, which was substantially lower. The diagonals changed less than the off-diagonal elements, with the non-parametric diagonal elements being between 0.91 and 1.20 times the assortative matrix elements (with intra-Pacific interactions relatively increasing the most and intra Māori interactions relatively decreasing the most). The transmission rates and initial reproduction numbers remained similar.

3.2.3. Scenario analysis

Attack rates varied to differing degrees as a result of changes to model parameters. When setting ϵ to zero or setting each group's vaccination rate to the population average, there was a relatively small change to the attack rates (Figure 6). Conversely, when setting the transmission rates to the population average, there was a significant change to the

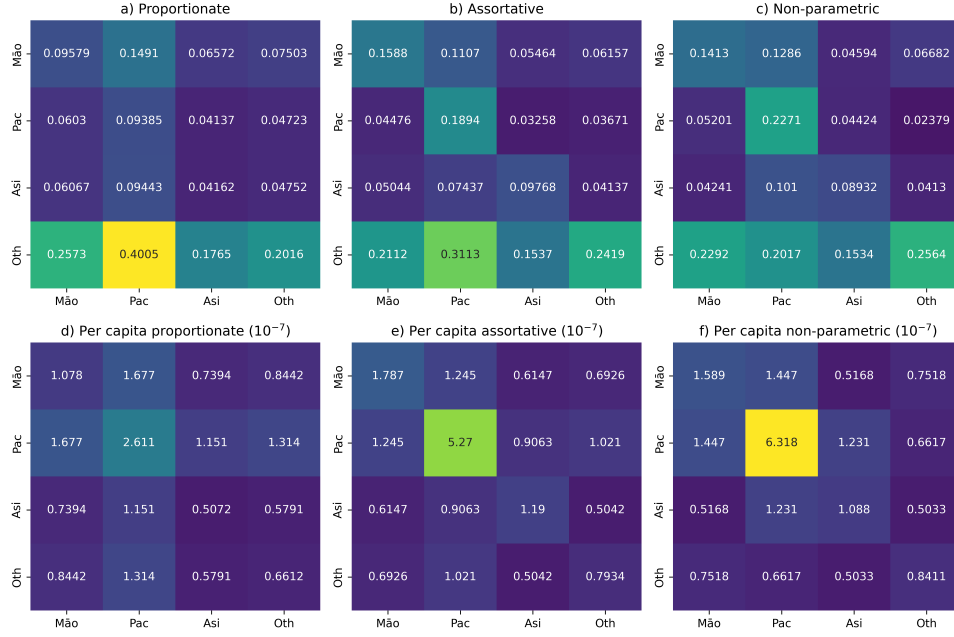


Figure 5. A comparison between a) the proportionate mixing transmission matrix; b) the assortative transmission matrix ($\epsilon = 0.179$); c) the non-parametric transmission matrix; d) the proportionate mixing per capita transmission matrix; e) the assortative per capita transmission matrix; and f) the non-parametric per capita transmission matrix. Matrices were fit with the prioritised SA2 population data (where relevant) such that the attack rates from the model matched the attack rates from the case data with an assumed CAR of 50%.

Table 3. Table of transmission rate values for prioritised SA2.

CAR	ϵ	a_k			
		Māori	Pacific	Asian	European/Other
Proportionate Mixing					
4060		0.589	1.001	0.230	0.261
40		0.528	0.899	0.344	0.396
50		0.474	0.738	0.325	0.371
60		0.446	0.669	0.314	0.357
Assortative Mixing					
4060	0.150	0.578	0.935	0.250	0.282
40	0.173	0.520	0.840	0.358	0.407
50	0.180	0.465	0.686	0.339	0.382
60	0.183	0.437	0.620	0.327	0.367
Non-parametric mixing					
4060		0.584	0.859	0.250	0.300
40		0.520	0.802	0.353	0.416
50		0.465	0.658	0.333	0.388
60		0.436	0.597	0.321	0.373

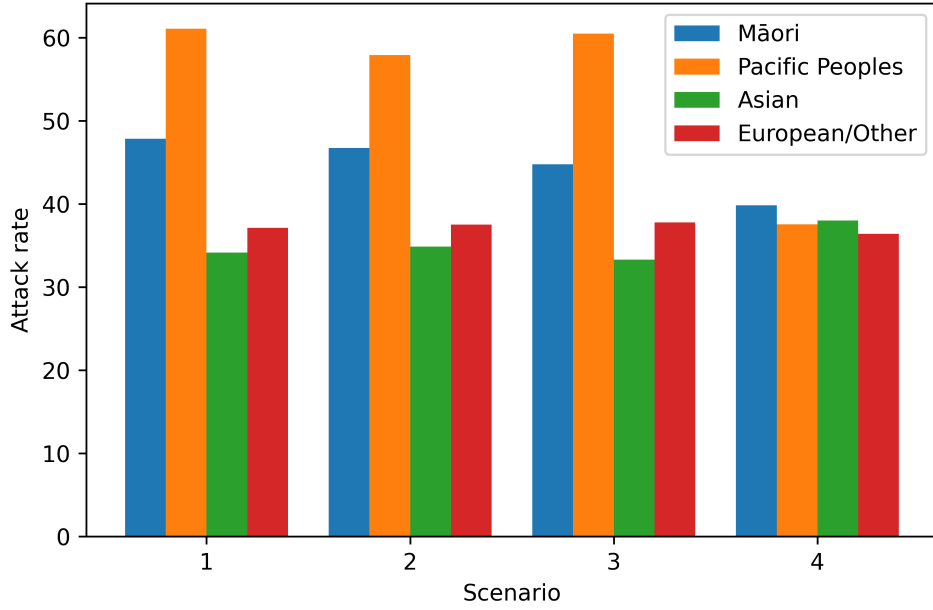


Figure 6. Comparison between the attack rates of the assortative mixing model with 1) no changes, 2) ϵ set to zero, 3) vaccination rates averaged, and 4) transmission rates averaged (see Table 2). The assortative matrix with no changes was fit to match the attack rates from the data with prioritised SA2 data and an assumed CAR of 50%. This meant the attack rates of 1) in the plot match the data. When the parameters were altered, the values were not refit.

attack rates; this showed the ethnic disparity in the number of infections was dominated by the disparity in transmission rates and not the assortativity value nor the disparity in vaccination rates. It is worth differentiating the effect of vaccines and the effect of the disparity in vaccination. Vaccines did have an effect on reducing incidence rate and, in the real world, substantially reduced mortality and severity of infection. The difference in vaccination coverage over ethnic groups had a relatively smaller effect on differences in attack rates by ethnicity compared to transmission rate differences. Similar results hold for total measure statistical area data, present in Appendix C.

4. Discussion

We explored the first Omicron wave during the COVID-19 pandemic in Aotearoa using an ethnicity-stratified SEIR model. We fit ethnicity-specific transmission rates and an assortativity constant such that the model’s attack rates matched those from the COVID-19 case data using three main assumptions of mixing: proportionate, assortative, and non-parametric mixing. We then attempted to quantify the relative importance of different drivers in the model.

Comparison of different scenarios revealed that, in our model, disparities in vaccination rates only explain a relatively small part of the observed differences in attack rates, so other factors must have been more important contributors. Likewise, assortative mixing alone is insufficient to explain these differences and can similarly only explain a relatively small difference. Differences between ethnicities in their average transmission rates explained a relatively large part of the observed differences, and therefore transmission rates are likely an important contributor. This is one possible explanation that

is consistent with the observed attack rate disparity.

To reproduce the ethnicity-specific attack rate data from Aotearoa’s first Omicron wave with an SEIR model required substantial differences in transmission rates between ethnicities. These transmission rates represent differences in social interactions and not biological responses, i.e., there is not a biological difference between ethnicities. Māori, Pacific Peoples, and Asians had transmission rates 1.28, 1.99, and 0.88 times higher than New Zealand Europeans under the assumption of proportionate mixing. This result was consistent with findings from Ma et al.; however, the relative differences in our transmission rates were slightly lower than for Ma et al. (2.25, 1.62, 0.86, and 1.28 times the non-Hispanic white rate in New York City for Hispanics or Latinos, non-Hispanic Black people, non-Hispanic Asians, and multiracial or other people, respectively) [23]. Like Ma et al., we found that relative differences between contact rates were smaller under the assumption of assortative mixing as opposed to proportionate mixing. ϵ was significantly lower than the Ma et al. value, being 18.0% instead of 46% in New York City. Reasons for these differences in the Aotearoa context, covered in the next paragraphs, could include workplace, average household occupancy, or age-distribution effects.

Work by Chang et al. has shown higher infection rates among disadvantaged racial and socioeconomic groups in part due to their inability to self-isolate as quickly as other groups [36]. This was partly due to workplace effects. Māori and Pacific Peoples were more likely to work in sectors or roles such as agriculture, transport, and manufacturing jobs [37]. While there were no lockdowns during the Omicron wave, these businesses would be operating close to normal levels during the first Omicron wave and would have less opportunity to work from home compared to other sectors. Risk would have also been increased working jobs that are more person-facing. A combination of these factors could have increased the risk and number of interactions Māori and Pacific Peoples faced during the first wave of Omicron.

Māori have historically been disadvantaged socio-economically, leading to worse health outcomes [38]. This disparity could be contributing to the disparity in transmission rates. In Switzerland, in 2021, adults and young adults living in higher socio-economic positions had fewer contacts than those in lower socio-economic positions. [39]. This would suggest socio-economic status could partly explain observed differences between ethnicities. Māori and Pacific Peoples typically have higher levels of deprivation that lead to an increased risk of hospitalisations from diseases such as influenza [40]. Deprivation is not only associated with the severity of infection but also the incidence rate of diseases. People who live in deprived areas are more likely to live in households with more people in them. Household crowding is a known risk factor for infectious diseases, like COVID-19, and disproportionately affects Māori, Pacific Peoples, and Asians [41,42]. In 2013, 20% of Māori, 38% of Pacific Peoples, and 18% of Asian people lived in crowded households, compared to just 4% of Europeans. In China, 75%-80% of clustered infections were within families, showing high intra-family transmission rates [34]. A meta-analysis of studies has estimated that the risk of household transmission is ten times that of other contacts [43]. Higher household crowding was one factor that probably contributed to higher transmission rates for the Māori and Pacific groups. The picture is less clear for the Asian group, as despite the increased rate of household crowding for Asians, our model estimated lower transmission rates. One possible reason for this was adherence to COVID-19 response measures in which Asians have been shown to have increased adherence to response measures such as contact tracing and mask wearing, both in Aotearoa [44,45] and overseas [46].

Māori and Pacific Peoples have a younger age distribution than Asian people and European/Others [47]. As a result, the average age of a case identifying as Māori will

be substantially lower than for European cases. Some studies have estimated that the majority of household transmissions begin with a child [48], and young adults are frequently estimated to have higher contact rates than older people [49,50]. This could contribute towards Māori and Pacific Peoples having higher transmission rates than European people. "Susceptibility to COVID-19 in individuals under 20 years of age has been estimated as half that of those over 20, which would mean Māori are expected to have fewer infections than European/Others. Another possible issue is that younger cases get reported less, as younger people manifest clinical symptoms less [22]. This could have led to fewer cases reported in younger populations, which would disproportionately affect Māori and Pacific Peoples and imply a lower CAR in these groups than for European/Other people.

In addition, other possible but less documented reasons for differences in transmission rates include differences in frequency of community interaction, method of transportation, and the cultural importance of interacting with extended family, which may be context-specific or hard to quantify. One example of cultural practices that could affect transmission rates was tangihanga, a Māori funeral practice, which contains a customary extended ceremony. During the pandemic, these ceremonies had measures to restrict COVID-19 spread, and at some points during the pandemic, tangihanga were not able to be held in any capacity [51]. During the Omicron wave, no more than 100 people were allowed into a marae, a traditional Māori tribal meeting place, at any one time. Strict COVID-19 measures were used at some marae to prevent transmission, despite this, tangihanga were still potential transmission events during Omicron [52]. As cultural activities were altered during COVID-19, it can be difficult to estimate the effect of these activities on disease transmission.

4.1. Sensitivity analysis

To analyse the sensitivity of our model, we varied the assumptions and data sources we used. The choice of CAR, data source for spatially disaggregated population sizes by ethnicity, and contact matrix method did not change the qualitative results from fitting the model. The value of CAR determines the magnitude of disparity but does not change the fact that disparity is present. A lower assumed CAR rate does lead to a greater disparity in the transmission rate, and when Māori and Pacific Peoples had a lower assumed CAR, the disparity in transmission rates was largest. Changing the assumed CAR did not change the relative ordering of transmission rates, i.e., Pacific Peoples always had the highest transmission rate. The values of transmission rates were not highly sensitive to whether we used population data from the Te Whatu Ora dataset or StatsNZ. These results were also not highly sensitive to whether we used SA1 or SA2 data. This shows that although quantitative estimates of model parameters differ, the qualitative conclusions are robust to the different data sources and assumptions tested.

4.2. Limitations

Our model ignores age-related effects and their interaction with ethnic effects, an obvious avenue for future work, which (as discussed above) could explain some of the observed disparities in attack rates. The same is true of combining other factors with ethnicity, such as deprivation/socioeconomic status. This is part of a larger limitation that we cannot definitively disentangle differences in transmission rates from differences in reporting rates or other factors. The main difference that drives disparity in COVID-

19 cases is likely to be transmission rates, but there could be other factors that are not included in the model. This is made more difficult to interpret by the fact that these ethnicity-specific transmission rates are proxies for a range of socioeconomic and cultural factors that affect contact patterns and transmission risk. We do not model a causation effect but a correlation between ethnicity and infection rate. These factors can change in complicated ways over time, which means estimates of contact patterns are restricted to the specific context of the first Omicron wave and may not generalise to other situations, e.g. non-pandemic periods or a future pandemic.

We also treat the first Omicron wave as a SEIR epidemic that ignores differences in time-dependent case rates, which are not well explained by a SEIR model. We fitted the model to data on reported cases with an assumption about how these relate to actual infections. We have investigated a scenario with lower CAR for Māori and Pacific Peoples, but this still assumes some measure of relationship between each ethnicity's CAR, which may or may not be representative of the real world. This could potentially be partly addressed in future work by including hospitalisations and deaths in the model, which are less sensitive to test-seeking behaviour (though they are sensitive to other differences, e.g. in rates of comorbidity).

Our model did not account for mixed ethnicities and used exclusive ethnic groups. The selection of exclusive ethnic groups was a crude approach, as it failed to account for multicultural people who may be affected by different socioeconomic variables and experience different epidemiological trends than any individual ethnic group. Within these groups there is a homogeneity assumption made to simplify modelling that does not account for intra-ethnic variation. One possible way to account for this would be to partition each combination of ethnicities into a separate group. This would represent multicultural individuals better. However, this could lead to group sizes with very few individuals in them that do not give much information, such as individuals who identify with all major ethnic groups.

Pacific Peoples, Asians, and Europeans/Others are underrepresented in prioritised datasets. For example, when the Ministry of Social Development swapped from a prioritised measure to a total measure, it saw the population identifying as Pacific and European rise from 9% to 12% and 39% to 53%, respectively [53]. Pacific Peoples are also historically underrepresented in the best available population data [54]. Both of these can lead to errors in estimates of model parameters, which are difficult to account for.

Our approach described a compartmental ethnicity-stratified model that we used to analyse ethnic transmission rates during the first Omicron wave in Aotearoa. Our model can be further developed to cover some of the limitations outlined and hopefully be used to inform policy on equitable pandemic decisions.

Acknowledgements

We are grateful to Kevin C. Ma and Stephen Kissler for their useful discussion about contact matrices.

Disclosure statement

We declare that we have no potential conflicts of interest with respect to the investigation, authorship, and publication of this article.

Funding

This work was supported by the Ngāi Tahu Research Centre, Canterbury University and Te Niwha Infectious Diseases Research Platform, Institute of Environmental Science and Research, grant number TN/P/24/UoC/MP and the Marsden Fund, grant number 24-UOC-020.

References

- [1] Jones R. Why equity for Māori must be prioritised during the Covid-19 response ; 2020. Section: Ātea; Available from: <https://thespinoff.co.nz/atea/18-03-2020/why-equity-for-maori-must-be-prioritised-during-the-covid-19-response>.
- [2] Steyn N, Binny RN, Hannah K, et al. Estimated inequities in COVID-19 infection fatality rates by ethnicity for Aotearoa New Zealand. *The New Zealand Medical Journal*. 2020 Sep;133(1521):28–39.
- [3] King P, Cormack D, McLeod M, et al. COVID-19 and Māori health – when equity is more than a word. *Public Health Expert Briefing*. 2020 Apr; Available from: <https://www.phcc.org.nz/briefing/covid-19-and-maori-health-when-equity-more-word>.
- [4] Whitehead J, Gan H, Heerikhuisen J, et al. Inequities in COVID-19 Omicron infections and hospitalisations for Māori and Pacific people in Te Manawa Taki Midland region, New Zealand. *Epidemiology and Infection*. 2023 Apr;151:e74.
- [5] Rice GW. Remembering 1918: Why Did Māori Suffer More than Seven Times the Death Rate of Non-Māori New Zealanders in the 1918 Influenza Pandemic? *New Zealand Journal of History*. 2019;53(1):90–108. Publisher: University of Auckland; Available from: <https://muse.jhu.edu/pub/426/article/883329>.
- [6] Wilson N, Barnard LT, Summers JA, et al. Differential Mortality Rates by Ethnicity in 3 Influenza Pandemics Over a Century, New Zealand. *Emerging Infectious Diseases*. 2012 Jan;18(1):71–77. Available from: <https://www.ncbi.nlm.nih.gov/pmc/articles/PMC3310086/>.
- [7] E/S/R. Measles weekly reports - 2019 ; 2019. Available from: <https://www.esr.cri.nz/digital-library/measles-weekly-reports-2019/>.
- [8] Chapple S. Death and disease at the dawn of New Zealand’s history. *The Turnbull Library record*. 2018 Sep;50.
- [9] Bennett J, Zhang J, Leung W, et al. Rising Ethnic Inequalities in Acute Rheumatic Fever and Rheumatic Heart Disease, New Zealand, 2000–2018. *Emerging Infectious Diseases journal*. 2021;27(1). Available from: https://wwwnc.cdc.gov/eid/article/27/1/19-1791_article.
- [10] Cheung IMY, Paynter J, Broderick D, et al. Severe Acute Respiratory Infection (SARI) due to Influenza in Post-COVID Resurgence: Disproportionate Impact on Older Māori and Pacific Peoples. *Influenza and Other Respiratory Viruses*. 2024;18(11):e70029. _eprint: <https://onlinelibrary.wiley.com/doi/pdf/10.1111/irv.70029>; Available from: <https://onlinelibrary.wiley.com/doi/abs/10.1111/irv.70029>.
- [11] Baker MG, Wilson N, Anglemeyer A. Successful Elimination of Covid-19 Transmission in New Zealand. *New England Journal of Medicine*. 2020 Aug;383(8):e56. Publisher: Massachusetts Medical Society _eprint: <https://www.nejm.org/doi/pdf/10.1056/NEJMc2025203>; Available from: <https://www.nejm.org/doi/full/10.1056/NEJMc2025203>.
- [12] Ministry of Health NZ. Managing COVID-19 in New Zealand ; 2024. Available from: <https://www.health.govt.nz/strategies-initiatives/programmes-and-initiatives/covid-19/managing-covid-19-in-new-zealand>.
- [13] Ardern J. First batch of COVID-19 vaccine arrives in NZ | Beehive.govt.nz ; 2021. Available from: <https://www.beehive.govt.nz/release/>

- first-batch-covid-19-vaccine-arrives-nz.
- [14] Parliamentary counsel office. COVID-19 Public Health Response (Protection Framework) Order 2021 ; 2021. Available from: <https://www.legislation.govt.nz/regulation/public/2021/0386/latest/whole.html#LMS595019>.
 - [15] Ministry of Health. New Zealand COVID-19 data ; 2023. Available from: <https://github.com/minhealthnz/nz-covid-data/>.
 - [16] Douglas J, Winter D, McNeill A, et al. Tracing the international arrivals of SARS-CoV-2 Omicron variants after Aotearoa New Zealand reopened its border. *Nature Communications*. 2022 Oct;13(1):6484. Available from: <https://doi.org/10.1038/s41467-022-34186-9>.
 - [17] Bowen JE, Addetia A, Dang HV, et al. Omicron spike function and neutralizing activity elicited by a comprehensive panel of vaccines. *Science*. 2022 Aug;377(6608):890–894. Publisher: American Association for the Advancement of Science; Available from: <https://www.science.org/doi/10.1126/science.abq0203>.
 - [18] Williamson EJ, Walker AJ, Bhaskaran K, et al. OpenSAFELY: factors associated with COVID-19 death in 17 million patients. *Nature*. 2020 Aug;584(7821):430–436. Available from: <https://www.ncbi.nlm.nih.gov/pmc/articles/PMC7611074/>.
 - [19] Goodfellow L, van Leeuwen E, Eggo RM. COVID-19 inequalities in England: a mathematical modelling study of transmission risk and clinical vulnerability by socioeconomic status. *BMC Medicine*. 2024 Apr;22(1):162. Available from: <https://doi.org/10.1186/s12916-024-03387-y>.
 - [20] Lyra W, Jr JDdN, Belkhiria J, et al. COVID-19 pandemics modeling with modified determinist SEIR, social distancing, and age stratification. The effect of vertical confinement and release in Brazil. *PLOS ONE*. 2020 Sep;15(9):e0237627. Publisher: Public Library of Science; Available from: <https://journals.plos.org/plosone/article?id=10.1371/journal.pone.0237627>.
 - [21] Miller IF, Becker AD, Grenfell BT, et al. Disease and healthcare burden of COVID-19 in the United States. *Nature Medicine*. 2020 Aug;26(8):1212–1217. Publisher: Nature Publishing Group; Available from: <https://www.nature.com/articles/s41591-020-0952-y>.
 - [22] Davies NG, Klepac P, Liu Y, et al. Age-dependent effects in the transmission and control of COVID-19 epidemics. *Nature Medicine*. 2020 Aug;26(8):1205–1211. Publisher: Nature Publishing Group; Available from: <https://www.nature.com/articles/s41591-020-0962-9>.
 - [23] Ma KC, Menkir TF, Kissler S, et al. Modeling the impact of racial and ethnic disparities on COVID-19 epidemic dynamics. *eLife*. 2021 May;10:e66601. Publisher: eLife Sciences Publications, Ltd; Available from: <https://doi.org/10.7554/eLife.66601>.
 - [24] Lee KK, Norris ET, Rishishwar L, et al. Ethnic disparities in mortality and group-specific risk factors in the UK Biobank. *PLOS Global Public Health*. 2023 Feb;3(2):e0001560. Available from: <https://www.ncbi.nlm.nih.gov/pmc/articles/PMC10021328/>.
 - [25] Datta S, Gilmour J, Harvey E, et al. Modelling the effect of changes to the COVID-19 case isolation policy. Covid-19 Modelling Aotearoa; 2023. Available from: <https://www.covid19modelling.ac.nz/modelling-the-effect-of-changes-to-the-covid-19-case-isolation-policy/>.
 - [26] Rosenstrom ET, Ivy JS, Mayorga ME, et al. COVSIM: A stochastic agent-based COVID-19 SIMulation model for North Carolina. *Epidemics*. 2024 Mar;46:100752. Available from: <https://www.sciencedirect.com/science/article/pii/S1755436524000136>.
 - [27] Park SW, Sun K, Abbott S, et al. Inferring the differences in incubation-period and generation-interval distributions of the Delta and Omicron variants of SARS-CoV-2. *Proceedings of the National Academy of Sciences*. 2023 May;120(22):e2221887120. Publisher: Proceedings of the National Academy of Sciences; Available from: <https://www.pnas.org/doi/10.1073/pnas.2221887120>.
 - [28] Cromer D, Steain M, Reynaldi A, et al. Predicting vaccine effectiveness against severe COVID-19 over time and against variants: a meta-analysis. *Nature Communications*.

- 2023 Mar;14(1):1633. Publisher: Nature Publishing Group; Available from: <https://www.nature.com/articles/s41467-023-37176-7>.
- [29] StatsNZ. Statistical area 1 dataset for 2018 Census – updated March 2020 ; 2020. Available from: <https://www.stats.govt.nz/information-releases/statistical-area-1-dataset-for-2018-census-updated-march-2020>.
- [30] Te Whatu Ora. COVID-19 Trends and Insights ; 2025. Available from: <https://tewhatauora.shinyapps.io/covid19/>.
- [31] Te Whatu Ora. Populations web tool ; 2023. Available from: <https://tewhatauora.shinyapps.io/populations-web-tool/>.
- [32] Watson LM, Plank MJ, Armstrong BA, et al. Jointly estimating epidemiological dynamics of Covid-19 from case and wastewater data in Aotearoa New Zealand. *Communications Medicine*. 2024 Jul;4(1):1–9. Publisher: Nature Publishing Group; Available from: <https://www.nature.com/articles/s43856-024-00570-3>.
- [33] StatsNZ. Statistical standard for geographic areas 2023 (updated December 2023). StatsNZ; 2023. Available from: <https://www.stats.govt.nz/methods/statistical-standard-for-geographic-areas-2023/>.
- [34] Chen S, Zhang Z, Yang J, et al. Fangcang shelter hospitals: a novel concept for responding to public health emergencies. *The Lancet*. 2020 Apr;395(10232):1305–1314. Publisher: Elsevier; Available from: [https://www.thelancet.com/journals/lancet/article/PIIS0140-6736\(20\)30744-3/fulltext](https://www.thelancet.com/journals/lancet/article/PIIS0140-6736(20)30744-3/fulltext).
- [35] lomas v. Vincentlomas/Modelling-the-interaction-between-ethnicity-and-infectious-disease-transmission-dynamics ; 2025. Original-date: 2025-07-10T01:01:21Z; Available from: <https://github.com/Vincentlomas/Modelling-the-interaction-between-ethnicity-and-infectious-disease-transmission-dynamics>.
- [36] Chang S, Pierson E, Koh PW, et al. Mobility network models of COVID-19 explain inequities and inform reopening. *Nature*. 2021 Jan;589(7840):82–87. Publisher: Nature Publishing Group; Available from: <https://www.nature.com/articles/s41586-020-2923-3>.
- [37] Harvey E, Hobbs M, Kvalsvig A, et al. A Summary of Risk Factors for COVID-19 Infection in Aotearoa New Zealand. *Covid-19 Modelling Aotearoa*; 2023. Available from: <https://www.covid19modelling.ac.nz/a-summary-of-risk-factors-for-covid-19-infection-in-aotearoa-new-zealand/>.
- [38] Robson B, Cormack D, Cram F. SOCIAL AND ECONOMIC INDICATORS. In: Hauora: Māori Standards of Health IV: A study of the years 2000-2005. Wellington: Te Rōpū Rangahau Hauora a Eru Pōmare; 2007. p. 21–32.
- [39] Domenico LD, Reichmuth ML, Althaus CL. Individual-based and neighbourhood-based socio-economic factors relevant for contact behaviour and epidemic control ; 2025. Pages: 2025.03.24.25324502; Available from: <https://www.medrxiv.org/content/10.1101/2025.03.24.25324502v1>.
- [40] Lopez L, Wood T, Prasad N, et al. Influenza surveillance in New Zealand 2016. Institute of Environmental Science and Research Ltd (ESR); 2016. Report. Available from: <https://apo.org.au/node/133116>.
- [41] Ministry of Health. Analysis of Household Crowding based on Census 2013 data. Ministry of Health. 2014;.
- [42] Johnson A, Howden-Chapman P, Eaquad S. A Stocktake Of New Zealand’s Housing. New Zealand Centre for Sustainable Cities. 2018;.
- [43] Lei H, Xu X, Xiao S, et al. Household transmission of COVID-19-a systematic review and meta-analysis. *The Journal of Infection*. 2020 Dec;81(6):979–997. Available from: <https://www.ncbi.nlm.nih.gov/pmc/articles/PMC7446647/>.
- [44] Chambers T, Anglemeyer A, Chen ATY, et al. An evaluation of the COVID-19 self-service digital contact tracing system in New Zealand. *Health Policy*. 2024 Jun;144:105073. Available from: <https://www.sciencedirect.com/science/article/pii/S0168851024000836>.
- [45] Gray L, MacDonald C, Tassell-Matamua N, et al. Wearing one for the team: views and

- attitudes to face covering in New Zealand/Aotearoa during COVID-19 Alert Level 4 lockdown. *Journal of Primary Health Care*. 2020 Sep;12(3):199–206. Publisher: CSIRO PUBLISHING; Available from: <https://www.publish.csiro.au/hc/HC20089>.
- [46] Hearne BN, Niño MD. Understanding How Race, Ethnicity, and Gender Shape Mask-Wearing Adherence During the COVID-19 Pandemic: Evidence from the COVID Impact Survey. *Journal of Racial and Ethnic Health Disparities*. 2022 Feb;9(1):176–183. Available from: <https://doi.org/10.1007/s40615-020-00941-1>.
- [47] Bryant J. The Ageing of the New Zealand Population, 1881-2051. New Zealand Treasury Working Paper; 2003. Working Paper 03/27. Available from: <https://www.econstor.eu/handle/10419/205532>.
- [48] Tseng YJ, Olson KL, Bloch D, et al. Smart Thermometer-Based Participatory Surveillance to Discern the Role of Children in Household Viral Transmission During the COVID-19 Pandemic. *JAMA Network Open*. 2023 Jun;6(6):e2316190. Available from: <https://doi.org/10.1001/jamanetworkopen.2023.16190>.
- [49] Prem K, Cook AR, Jit M. Projecting social contact matrices in 152 countries using contact surveys and demographic data. *PLOS Computational Biology*. 2017 Sep;13(9):e1005697. Publisher: Public Library of Science; Available from: <https://journals.plos.org/ploscompbiol/article?id=10.1371/journal.pcbi.1005697>.
- [50] Hoang T, Coletti P, Melegaro A, et al. A Systematic Review of Social Contact Surveys to Inform Transmission Models of Close-contact Infections. *Epidemiology*. 2019 Sep;30(5):723. Available from: https://journals.lww.com/epidem/fulltext/2019/09000/a_systematic_review_of_social_contact_surveys_to.15.aspx.
- [51] Rangiwhai B, Sciascia A. The Impacts of COVID-19 on Tangihanga. *Journal of Global Indigeneity*. 2021 Feb;5(1):1–14. Publisher: Bronwyn Carlson; Available from: <https://www.journalofglobalindigeneity.com/article/19435-the-impacts-of-covid-19-on-tangihanga>.
- [52] Cooper K. Covid 19 Omicron outbreak: Positive case visited Far North marae for tangihanga ; 2022. Section: Northern Advocate; Available from: <https://www.nzherald.co.nz/northern-advocate/news/covid-19-omicron-outbreak-positive-case-visited-far-north-marae-for-tangihanga/YHAW47R6KTQYXHIDWLH6AVQKVU/>.
- [53] Ministry of Social Development. Improving how we report ethnicity ; 2021. Available from: <https://www.msd.govt.nz/about-msd-and-our-work/tools/how-we-report-ethnicity.html>.
- [54] Sonder GJ, Grey C, Ryan D, et al. Selective under-representation of Pacific peoples in population estimates for health indicator measurements in Aotearoa New Zealand misinforms policy making. *BMC Public Health*. 2024 Feb;24(1):564. Available from: <https://doi.org/10.1186/s12889-024-17984-2>.

Appendix A. Statistical area information

Table A1 contains various statistics about the statistical area datasets used in parameter fitting.

Appendix B. Parameter Variation

In Figure B1, the transmission rates were held constant to the values fit to the proportionate mixing scheme while ϵ varied. This was done without the effect of vaccines considered (i.e. vaccinated population as set to zero). As can be seen, the disparity in attack rate between groups widened as ϵ increased. This was expected, as when epsilon

Table A1. Table of various statistical measures of the ethnic populations within the SA datasets, where SD is the standard deviation of the populations, and interquartile range is the range between the 75th and 25th quartile of the population sizes.

	Total	Mean	Median	SD	Range	Interquartile range
SA1 Total measure						
Māori	775410	26.5	18.0	28.2	0 - 435	9 - 33
Pacific Peoples	381576	13.0	6.0	25.4	0 - 315	0 - 12
Asians	707499	24.2	12.0	33.4	0 - 789	3 - 33
Europeans/Others	3424572	117.0	114.0	49.8	0 - 825	84 - 147
All ethnicities	5289057	180.7	174.0	60.4	27 - 1188	141 - 213
SA2 Total measure						
Māori	775875	362.6	252.0	355.7	0 - 3477	138 - 472
Pacific Peoples	381711	178.4	60.0	381.4	0 - 3501	24 - 138
Asians	707541	330.6	126.0	467.6	0 - 4530	45 - 414
Europeans/Others	3425964	1600.9	1539.0	827.3	9 - 4230	995 - 2136
All ethnicities	5291091	2472.5	2395.5	1243.7	33 - 6099	1518 - 3319
SA2 Priority measure						
Māori	888840	412.1	290.0	396.6	0 - 3780	160 - 540
Pacific Peoples	359480	166.7	50.0	376.7	0 - 3440	20 - 120
Asians	820580	380.4	150.0	534.0	0 - 5760	50 - 470
Europeans/Others	3048470	1413.3	1330.0	821.0	10 - 7600	830 - 1910
All ethnicities	5117370	2372.4	2300.0	1215.5	10 - 10120	1470 - 3170

approached one, different ethnicities' equations decoupled into separate SEIR models, which had no dependence on other ethnicities transmission rates. ϵ was also varied while the transmission rates were refit to the attack rate data (under the assumed value for CAR). It would not be qualitatively reasonable if the gap between the times of the peak positions was too large and values over 0.6 tend to not have qualitatively reasonable gaps in peak timing.

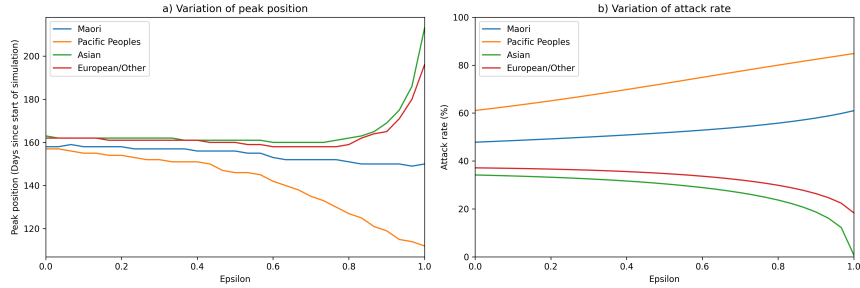


Figure B1. a) Plot of the time of the peak position of new infections for each ethnicity while varying ϵ . The transmission vector, \mathbf{a} , was refit to the attack rates from the data for every value of epsilon plotted, such that every point on the graph was from a model that matched the attack rates from the data. b) Plot of attack rate values with variation of ϵ . The transmission vector, \mathbf{a} , was fit to the attack rates from the data with an assumed CAR of 50% and no assortativity (i.e., pure proportional mixing).

Appendix C. Results for total measure SA1 and SA2 data

Values of the transmission rates fit to the SA1 and SA2 total measure population projections can be seen in Table C1.

Figures C1 compare the assortative transmission matrices fit using the total measure

Table C1. Table of transmission rate values fit using the assortative mixing model for total population data.

CAR	ϵ	a_k			
		Māori	Pacific	Asian	European/Other
SA1					
4060	0.163	0.577	0.929	0.252	0.284
40	0.185	0.519	0.836	0.359	0.408
50	0.192	0.465	0.682	0.340	0.382
60	0.195	0.436	0.617	0.328	0.367
SA2					
4060	0.123	0.580	0.947	0.246	0.278
40	0.152	0.521	0.846	0.357	0.406
50	0.158	0.466	0.692	0.337	0.380
60	0.161	0.438	0.626	0.325	0.365

population data. Figures C2 and C3 show quantification analysis results for the total measure statistical area datasets.



Figure C1. Comparison between the assortative mixing transmission matrices fit using a) SA1 total population data and b) SA2 total population data. Matrices were fit to the attack rate data with an assumed CAR of 50%.

Figures C2 and C3 show quantification analysis repeated for the total population measures.

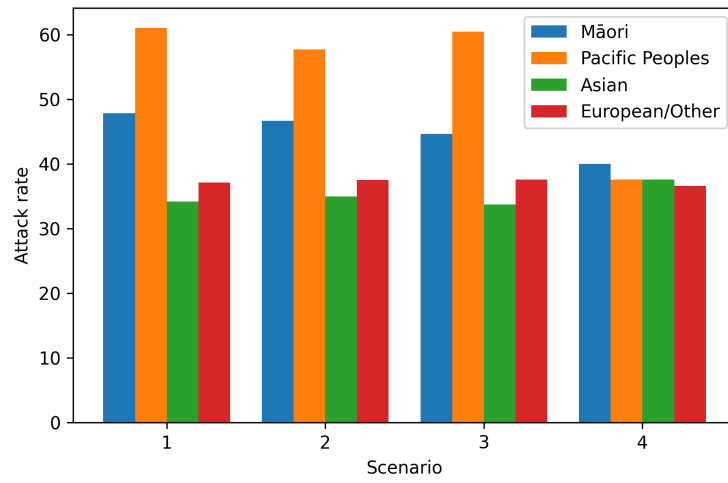


Figure C2. Quantification analysis using SA1 total measure population data. The four scenarios considered are: 1) ethnicity-specific parameters and assortativity, 2) no assortativity, 3) population-averaged vaccination rates, 4) population-averaged transmission rates.

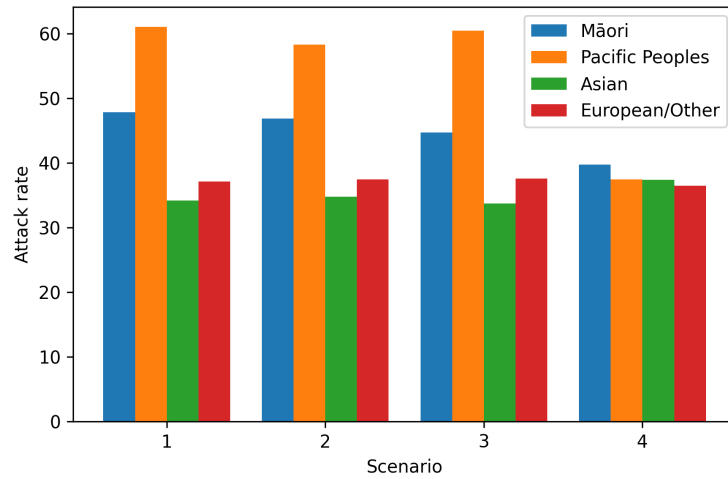


Figure C3. Quantification analysis using SA2 total measure population data. The four scenarios considered are: 1) ethnicity-specific parameters and assortativity, 2) no assortativity, 3) population-averaged vaccination rates, 4) population-averaged transmission rates.